Research Article

Effect of Binary Hybrid Nanofluid Flow Between Parallel Plates With Applied Activation Energy

Ramesh Alluguvelli[1] , Balla Chandra Shekar*[2] , Khasim Ali[3] and
Rayaprolu Chandra Shekhar[4]

[1] *Department of Mathematics, Geethanjali College of Engineering and Technology, Cheeryal, Hyderabad, Telangana, India*

[2] *Department of Mathematics, Sreenidhi University, Yamnapet, Ghatkesar, Hyderabad 501301, Telangana, India*

[3] *Department of Mathematics, Nawab Shah Alam Khan College of Engineering and Technology, Hyderabad, Telangana, 500024, India*

[4] *Department of Mathematics, Vignana Bharathi Institute of Technology, Aushapur, Hyderabad, Telangana, India*

*Corresponding author: shekar.balla@gmail.com

Abstract. This article examines the activation energy between two parallel plates consisting of MoS_2-GO-EO hybrid nanofluid. The nanoparticles, *molybdenum disulphide* (MoS_2) and *graphene oxide* (GO), are added to the base fluid, engine oil (EO). The influence of activation energy is also measured in this model. The finite difference method (FDM) is used to integrate the equations of motion, heat, and mass balance. The effects of important parameters such as activation energy, chemical reaction, temperature difference, random motion, and thermophoresis are discussed. The Nusselt number and skin friction are compared with available work to validate the numerical procedure. An enhanced Sherwood number is observed in Buongiorno's nanofluid model, while an elevated Nusselt number is seen with the hybrid nanofluid. Activation energy increases the profiles of temperature and concentration.

Keywords. Hybrid nanofluid, Activation energy, Brownian motion, Thermophoresis, Flow between two plates, Two phase nanofluid model

Mathematics Subject Classification (2020). 76M20, 76R10, 80M20

1. Introduction

Svante Arrhenius [5] first introduced the concept of activation energy in 1889. Activation energy is the minimum energy required for a material to initiate a reaction. The process has gained considerable attention owing to its diverse applications in industrial engineering, base liquid mechanics, recovering thermal oil, etc. Bestman [6] was the first to investigate the combined effects of a chemical reaction and Arrhenius activation energy on convective mass transfer in a vertically oriented porous pipe. He utilized perturbation method to acquire an analytical solution. Zeeshan *et al.* [32] examined the activation energy in magnetohydrodynamics (MHD) radiative Couette-Poiseuille flow of nanofluid in horizontally oriented channel under convective boundary constraints. Makinde and Franks [19] investigated hydromagnetic reactive unsteady Couette flow with activation energy. Mustafa *et al.* [23] studied the impact of activation energy in the nanofluid flow and heat transfer past an exponentially stretched sheet. Bodduna *et al.* [8] considered activation energy in bioconvective nanoliquid flow in cavity.

Choi and Eastman [10] were instrumental in popularizing the term "nanofluid" to describe the homogeneous suspension of nanoparticles within a base liquid. Because of the diverse thermal applications of nanoparticles, researchers have recognized numerous applications for these tiny particles in industrial processes, engineering systems, and practical challenges. There are two models utilized by many researchers to describe nanofluid flow. The properties of nanoparticles are focussed in the first model, known as single phase nanofluid model. This model is focussed by Biswas *et al.* [7], Khanafer and Vafai [16], and Tiwari and Das [30]. Saha and Paul [24] investigated turbulent flow of water-based Al_2O_3 and TiO_2 NFs in a pipe subject to a constant heat flux boundary constraint. They employed single-phase (homogeneous) technique and thermo-reliant properties. Manca *et al.* [20] inspected nanofluid convection of Al_2O_3/H_2O in 2-D channel with uniform heat flux by using single-phase. Ahmed *et al.* [2] examined convective heat transfer through pipe under fixed wall thermal conditions.

Alternatively, the second model, known as the two-phase model proposed by Buongiorno [9], incorporates Brownian motion and thermophoresis, treating the concentration of nanoparticles as inhomogeneous. Gorla *et al.* [12], Mahmoodi and Kandelousi [18], Motlagh and Soltanipour [22], Sheremet and Pop [26], and Sheremet *et al.* [27] addressed this model. Ali and Makinde [3] investigated Buongiorno's Couette nanofluid flow. Karim *et al.* [15] inspected the impact of copper-water nanofluid flow through Couette channel. Meenakshi *et al.* [21] studied influence of Brownian motion and thermophoresis on nanofluid flow. Hybrid nanofluid, a versatile substance utilized across various fields of high technology such as manufacturing, electro-sensing, thermal biosensors, and acoustic wave sensors, is created through the amalgamation of multiple types of nanoparticles within a base liquid suspension (see Ali [1], Huminic and Huminic [14], and Sidik *et al.* [28]). Sheikholeslami *et al.* [25] inspected impacts of heat transfer, mass transfer of unsteady fluid flow past two plates. In their study, Ghalambaz *et al.* [11] inspected the flow of hybrid nanofluid in square cavity. Sundar *et al.* [29] analyzed hybrid nanofluid consisting of $MWCNT–Fe_3O_4/H_2O$, whereas Madhesh *et al.* [17] conducted an analysis of copper-titania/water hybrid nanofluid.

The objective of this article is to investigate the transient two-dimensional flow occurring between two parallel plates, using a two-phase nanofluid model concerning activation energy.

The channel is intended to accommodate a blend of nanoparticles, molybdenum disulphide and graphene oxide in the base fluid of engine oil. As far as the authors are aware, the efficacy of activation energy in the channel flow of a hybrid nanofluid composed of molybdenum disulphide, graphene oxide, and engine oil has not been explored. By employing finite difference method, the given equations are solved, and the resulting outcomes are visually represented through 2-D contours that depict the flow characteristics, as well as the distributions of heat and volume fractions.

2. Mathematical Formulation

Consider a flow configuration between two parallel plates, where the base fluid Engine Oil (EO) is augmented with hybrid nanoparticles Molybdenum Disulphide-Graphene Oxide (MoS$_2$-GO). In this investigation, we also take into account the influence of activation energy. In Figure 1, x-axis is regarded to align with wall, while y-axis is assumed to be perpendicular to it. At the top plate ($y = h$), a convective condition is taken into consideration. Table 1 illustrates the thermophysical properties of both the nanoparticles and the base fluid. The equations governing the system, which are based on the NF approaches proposed by Buongiorno [9], and Tiwari and Das [30], are as follows:

$$\frac{\partial u}{\partial x} = 0, \tag{2.1}$$

$$\rho_{hnf}\frac{\partial u}{\partial \bar{t}} = -\frac{\partial \bar{P}}{\partial x} + \mu_{hnf}\frac{\partial^2 u}{\partial y^2}, \tag{2.2}$$

$$\frac{\partial \bar{T}}{\partial \bar{t}} = \alpha_{hnf}\frac{\partial^2 \bar{T}}{\partial y^2} + \frac{\mu_{hnf}\,\alpha_{hnf}}{k_{hnf}}\left(\frac{\partial u}{\partial y}\right)^2 + \tau\left[D_B\left(\frac{\partial \bar{T}}{\partial y}\frac{\partial \bar{C}}{\partial y}\right) + \frac{D_T}{T_a}\left(\frac{\partial \bar{T}}{\partial y}\right)^2\right], \tag{2.3}$$

$$\frac{\partial \bar{C}}{\partial \bar{t}} = D_B\frac{\partial^2 \bar{C}}{\partial y^2} + \frac{D_T}{T_a}\frac{\partial^2 \bar{T}}{\partial y^2} - Kr^2(\bar{C} - \bar{C}_0)\left(\frac{\bar{T}}{\bar{T}_0}\right)^n\exp\left(\frac{-E_a}{\kappa\bar{T}}\right). \tag{2.4}$$

The boundary conditions are given by,

$$u = 0, \quad \bar{T} = \bar{T}_0, \quad \bar{C} = \bar{C}_0, \quad \text{at } y = 0,$$

$$u = U_h, \quad -k_{hnf}\frac{\partial \bar{T}}{\partial y} = h_f(\bar{T} - \bar{T}_\infty), \quad D_B\frac{\partial \bar{C}}{\partial y} = -\frac{D_T}{T_\infty}\frac{\partial \bar{T}}{\partial y}, \quad \text{at } y = h.$$
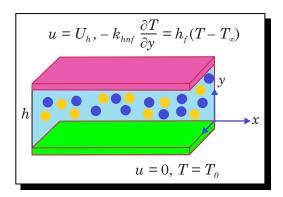

Figure 1. Physical configuration

The thermophysical attributes pertaining to both the nanofluid and hybrid nanofluid are detailed as follows

$$\mu_{nf} = \frac{\mu_f}{(1-\phi)^{2.5}},$$

$$\rho_{nf} = (1-\phi)\rho_f + \phi\rho_s,$$

$$\alpha_{nf} = \frac{\kappa_{nf}}{(\rho C_P)_{nf}},$$

$$(\rho C_P)_{nf} = (1-\phi)(\rho C_P)_f + \phi(\rho C_P)_s,$$

$$\frac{\kappa_{nf}}{\kappa_f} = \frac{(\kappa_{s1} + 2\kappa_f) - 2\phi_1(\kappa_f - \kappa_{s1})}{(\kappa_{s1} + 2\kappa_f) + \phi_1(\kappa_f - \kappa_{s1})},$$

$$\rho_{hnf} = \left\{ (1-\phi_2)\left((1-\phi_1) + \phi_1 \frac{\rho_{s1}}{\rho_f} \right) + \phi_2 \frac{\rho_{s2}}{\rho_f} \right\} \rho_f,$$

$$(\rho C_p)_{hnf} = \left\{ (1-\phi_2)\left((1-\phi_1) + \phi_1 \frac{(\rho C_p)_{s1}}{(\rho C_p)_f} \right) + \phi_2 \frac{(\rho C_p)_{s2}}{(\rho C_p)_f} \right\} (\rho C_p)_f,$$

$$\mu_{hnf} = \frac{\mu_f}{(1-\phi_1)^{2.5}(1-\phi_2)^{2.5}},$$

$$\kappa_{hnf} = \frac{(\kappa_{s2} + 2\kappa_f) - 2\phi_2(\kappa_f - \kappa_{s2})}{(\kappa_{s2} + 2\kappa_f) + \phi_2(\kappa_f - \kappa_{s2})}\kappa_{nf}.$$

Table 1. Thermophysical values of MoS_2, GO and EO

Physical properties	MoS_2	GO	EO
C_p (J/KgK)	397.21	717	1910
ρ (Kg/m^3)	5060	1800	884
k (W/mK)	904.4	5000	0.144

The following nondimensional parameters are utilized:

$$X = \frac{x}{h}, \ Y = \frac{y}{h}, \ U = \frac{u}{U_h} = \frac{hu}{\nu_f}, \ t = \frac{\bar{t}\nu_f}{h^2} = \frac{\tau U_h}{h}, \ \theta = \frac{\bar{T} - \bar{T}_0}{\bar{T}_\infty - \bar{T}_0}, \ \phi = \frac{\bar{C} - \bar{C}_0}{\bar{C}_\infty - \bar{C}_0},$$

$$\alpha_f = \frac{k_f}{(\rho C_P)_f}, \ P = \frac{\bar{P}h^2}{\rho_f \nu_f^2}, \ \omega = \frac{Kr^2 h^2}{\nu_f}, \ Ec = \frac{\nu_f^2}{C_P(\bar{T}_\infty - \bar{T}_0)h^2}, \ A = -\frac{\partial P}{\partial X}, \ Bi = \frac{hh_f}{k_f},$$

$$Pr = \frac{\nu_f}{\alpha_f}, \ \delta = \frac{\Delta C}{\bar{T}_o}, \ E = \frac{E_a}{\kappa \bar{T}_o}, \ Nb = \frac{\tau D_B(\bar{C}_\infty - \bar{C}_0)}{\alpha_f}, \ Nt = \frac{\tau D_T(\bar{T}_\infty - \bar{T}_0)}{T_\infty \alpha_f}, \ Sc = \frac{\nu_f}{D_B}.$$

The non-dimensional transformed equations are:

$$\frac{\partial U}{\partial t} = \frac{\rho_f}{\rho_{hnf}} \left\{ A + \frac{\mu_{hnf}}{\mu_f} \frac{\partial^2 U}{\partial Y^2} \right\}, \tag{2.5}$$

$$\frac{\partial T}{\partial t} = \frac{(\rho C_p)_f}{(\rho C_p)_{hnf}} \left\{ \frac{1}{Pr} \frac{k_{hnf}}{k_f} \frac{\partial^2 T}{\partial Y^2} + \frac{\mu_{hnf}}{\mu_f} Ec \left(\frac{\partial U}{\partial Y} \right)^2 \right\} + \frac{Nb}{Pr} \frac{\partial T}{\partial Y} \frac{\partial C}{\partial Y} + \frac{Nt}{Pr} \left(\frac{\partial T}{\partial Y} \right)^2, \tag{2.6}$$

$$\frac{\partial C}{\partial t} = \frac{1}{Sc}\left(\frac{\partial^2 C}{\partial Y^2} + \frac{Nt}{Nb}\frac{\partial^2 T}{\partial Y^2}\right) - \omega(1+\delta T)^2 C\exp\left(\frac{-E}{1+\delta T}\right). \tag{2.7}$$

The nondimensional boundary conditions are

When $t > 0$, $U = 0$, $T = 0$, $C = 1$, at $Y = 0$,

$$U = 1, \quad \frac{\partial T}{\partial Y} = -Bi(T-1), \quad \frac{\partial C}{\partial Y} = -\frac{Nt}{Nb}\frac{\partial T}{\partial Y}, \quad \text{at } Y = 1. \tag{2.8}$$

The parameters skin friction, Sherwood and Nusselt number at bottom, top walls are specified as

$$C_f = \frac{1}{(1-\phi_1)^{2.5}(1-\phi_2)^{2.5}}\frac{\partial U}{\partial Y}_{Y=0,1}, \quad Sh = -\frac{\partial C}{\partial Y}_{Y=0,1} \quad \text{and} \quad Nu = -\frac{k_{hnf}}{k_f}\frac{\partial \theta}{\partial Y}_{Y=0,1}.$$

3. Methodology of Solution

The governing nonlinear expressions (2.5)-(2.8) is were solved for numerical solution using FDM (Ali *et al.* [4], Ali and Makinde [3], Hajmohammadi [13], Karim *et al.* [15], Tlili *et al.* [31]). The 1st and 2nd order differentials are approached by forward and central differences, respectively. The convergence is accomplished when $|\varphi^{n+1} - \varphi^n| \leq 10^{-5}$, where n is frequency of instances and φ specifies $[U, \theta, \phi]$. Table 2 presents an analogy between current data to prior studies for special instance $\phi = 0$, and an excellent agreement is observed.

Table 2. Comparison of Skin friction and Nusselt number for $\phi = 0$

β	Bi	Cf			Nu		
		Ali and Makinde [3]	Karim *et al.* [15]	Current results	Ali and Makinde [3]	Karim *et al.* [15]	Current results
0.1	1	3.97×10^{-1}	3.95×10^{-1}	3.962×10^{-1}	5.12×10^{-1}	5.11×10^{-1}	5.121×10^{-1}
0.1	3	4.06×10^{-1}	4.05×10^{-1}	4.058×10^{-1}	7.90×10^{-1}	7.84×10^{-1}	7.883×10^{-1}
0.5	1	1.45×10^{-1}	1.46×10^{-1}	1.443×10^{-1}	2.23×10^{-1}	2.21×10^{-1}	2.227×10^{-1}

4. Discussion

This section focusses on presenting computational results of nanofluid flow between plates comprising molybdenum disulphide (MoS_2) and graphene oxide (GO) as nanoparticles and engine oil (EO) as base liquid. The outcomes are demonstrated in the form of contours and streamlines for quantities: activation energy ($E = 1-5$), nanoparticle volume fraction ($\phi = 0.01-0.25$), Biot number ($Bi = 1$), Eckert number ($Ec = 0.1-1$), Brownian movement ($Nb = 0.01-0.2$), thermophoretic parameter ($Nt = 0.01-0.5$), chemical reaction ($\omega = 0.1-3$) and temperature difference ($\delta = 0.1-3$).

Figure 2 depicts the profiles of velocity, temperature and concentration of nanoparticle concentration for the alteration of nanoparticle volume fraction (ϕ). In case of MoS_2-EO nanofluid, a rise in the nanoparticle volume fraction declines velocity and concentration in the channel. Conversely, the escalation in nanoparticle volume fraction improves the temperature. The figure also demonstrates that the enhancement/reduction trend caused by MoS_2-EO nanofluid is opposite to that of MoS_2-GO-EO hybrid nanofluid. The introduction of GO

nanoparticles enhances the thermal conductivity, resulting in an improvement in temperature in the case of hybrid nanofluid.
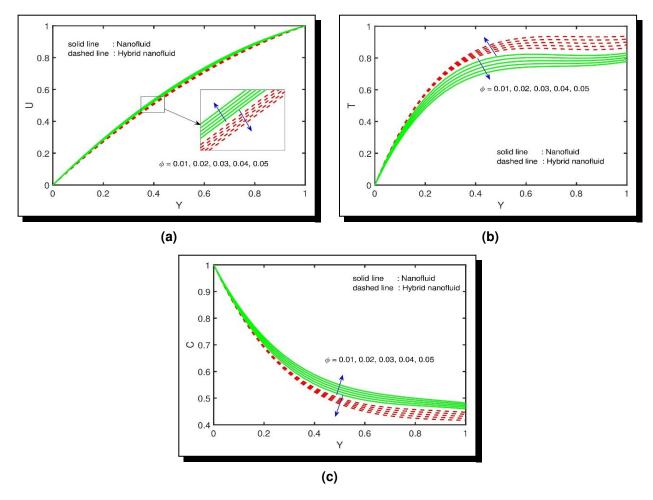

(a)

(b)

(c)

Figure 2. Effect of ϕ on (a) velocity, (b) temperature, (c) concentration for $E = 1$, $\omega = 1$, $\delta = 1$, $Ec = 1$, $Pr = 30$, $Bi = 1$, $Nb = 0.4$, $Nt = 0.16$, $Sc = 1$

(a)

(b)

Figure 3. Effect of δ on (a) temperature, (b) concentration for $E = 1$, $\omega = 1$, $\phi = 0.05$, $Ec = 1$, $Pr = 30$, $Bi = 1$, $Nb = 0.4$, $Nt = 0.16$, $Sc = 1$

Figure 3 illustrates the nanoparticle concentration and temperature trends as temperature difference (δ) varies. The growth in δ reduced the temperature and the concentration. Furthermore, it is evident that the impact of increasing δ on the reduction is more pronounced in the case of MoS_2-GO-EO hybrid nanofluid compared to MoS_2-EO nanofluid.

The profiles of temperature and nanoparticle concentration for the variation of activation energy (E) are depicted in Figure 4. The rise in E upsurges the concentration and temperature as well. The temperature trend is found to be advanced for MoS_2-GO-EO hybrid nanofluid compared to MoS_2-EO nanofluid. The concentration trend in MoS_2-GO-EO hybrid nanofluid is comparatively lower than that in MoS_2-EO nanofluid.
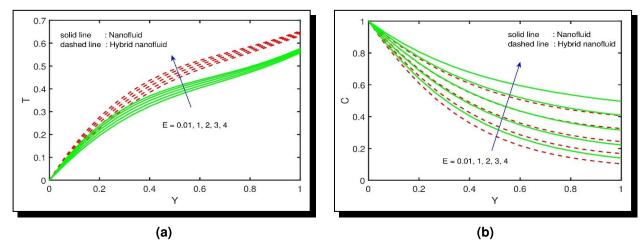

Figure 4. Effect of E on (a) temperature, (b) concentration for $\omega = 1$, $\delta = 1$, $\phi = 0.05$, $Ec = 1$, $Pr = 30$, $Bi = 1$, $Nb = 0.4$, $Nt = 0.16$, $Sc = 1$

Figure 5 describes the profile of nanoparticle concentration and temperature for the alteration of chemical reaction (ω). The rise in ω deteriorates the concentration and temperature in channel. The temperature trend indicates greater increase in MoS_2-GO-EO hybrid nanofluid compared to that observed in MoS_2-EO nanofluid. In contrast, concentration trend demonstrates opposite to that of temperature trend.
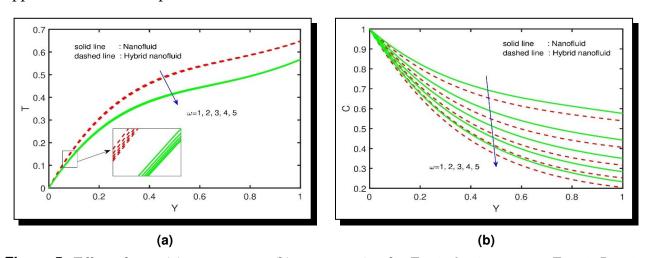

Figure 5. Effect of ω on (a) temperature, (b) concentration for $E = 1$, $\delta = 1$, $\phi = 0.05$, $Ec = 1$, $Pr = 30$, $Bi = 1$, $Nb = 0.4$, $Nt = 0.16$, $Sc = 1$

Figure 6 illustrates the profile of nanoparticle concentration and temperature for the alteration of Nb. The rise in Nb accelerates concentration of channel. Brownian motion induces a decrease in temperature within the channel. The temperature trend is found to be advanced for MoS_2-GO-EO hybrid nanofluid compared to MoS_2-EO nanofluid. The concentration profile for MoS_2-GO-EO hybrid nanofluid is found to be declined than that of MoS_2-EO.
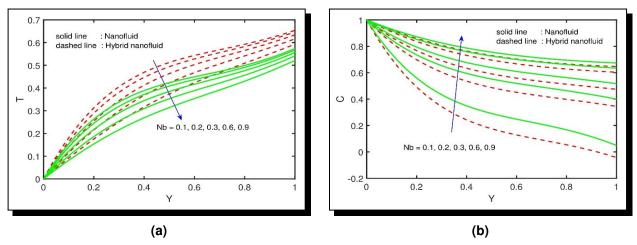

Figure 6. Effect of Nb on (a) temperature, (b) concentration for $E = 1$, $\omega = 1$, $\delta = 1$, $\phi = 0.05$, $Ec = 1$, $Pr = 30$, $Nt = 0.16$, $Bi = 1$, $Sc = 1$

Figure 7 illustrates the profile of nanoparticle concentration and temperature for the alteration of thermophoresis (Nt). The rise in thermophoresis accelerates the temperature and decelerates the concentration of channel. The temperature trend is found to be advanced in MoS_2-GO-EO hybrid nanofluid compared to MoS_2-EO nanofluid. The concentration trend is detected to be declined for MoS_2-GO-EO hybrid nanofluid than that of MoS_2-EO nanofluid.
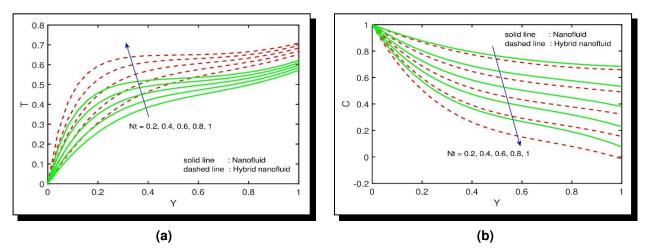

Figure 7. Effect of Nt on (a) temperature, (b) concentration for $E = 1$, $\omega = 1$, $\delta = 1$, $\phi = 0.05$, $Ec = 1$, $Pr = 30$, $Nb = 0.4$, $Bi = 1$, $Sc = 1$

Figure 8 displays Nu_{avg} and Sh_{avg} for alteration of Buongiorno model, NF, hybrid nanofluid and activation energy. As the activation energy grows from $E = 0.1$ to $E = 4$, Sherwood number Sh_{avg} decreases for Buongiorno model, MoS_2-EO nanofluid and MoS_2-GO-EO hybrid nanofluid.

Hybrid nanofluid model showed higher Sh_{avg}. In contrast, Nu_{avg} showed increasing trend for Buongiorno model, MoS_2-EO nanofluid and MoS_2-GO-EO hybrid nanofluid.
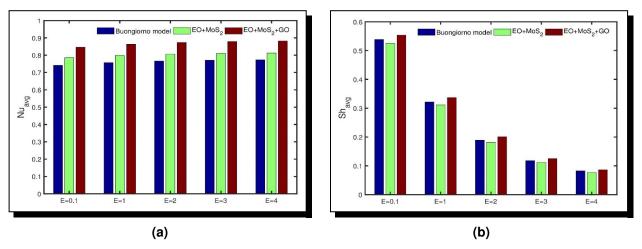

Figure 8. Effect of E on (a) Nusselt number, (b) Sherwood number for nanofluid and hybrid nanofluid

5. Conclusions

This article inspects the impacts of molybdenum disulphide-graphene oxide-engine oil hybrid nanofluid and molybdenum disulphide-engine oil nanofluid accompanying activation energy in flow of channel with parallel plates. FDM is functioned to execute the computation of outcomes. The inferences are drawn as follows:

- Velocity profile is weakened with nanoparticle volume fraction (ϕ).
- Temperature profile is boosted with activation energy (E), thermophoresis (Nt) and nanoparticle volume fraction (ϕ). In contrast, Brownian motion (Nb), temperature difference (δ) and chemical reaction parameter (ω) reduced the temperature profile.
- Nanoparticle concentration profile is deteriorated with thermophoresis (Nt), temperature difference (δ), chemical reaction parameter (ω), and nanoparticle volume fraction (ϕ). In contrast, activation energy (E) and Brownian motion (Nb) elevated the concentration profile.

Competing Interests

The authors declare that they have no competing interests.

Authors' Contributions

All the authors contributed significantly in writing this article. The authors read and approved the final manuscript.

References

[1] H. M. Ali, *Hybrid Nanofluids for Convection Heat Transfer*, 1st edition, Academic Press, London, 300 pages (2020), DOI: 10.1016/C2018-0-04602-2.

[2] M. A. Ahmed, M. M. Yaseen and M. Z. Yusoff, Numerical study of convective heat transfer from tube bank in cross flow using nanofluid, *Case Studies in Thermal Engineering* **10** (2017), 560 – 569, DOI: 10.1016/j.csite.2017.11.002.

[3] A. O. Ali and O. D. Makinde, Modelling the effect of variable viscosity on unsteady Couette flow of nanofluids with convective cooling, *Journal of Applied Fluid Mechanics* **8**(4) (2015), 793 – 802, DOI: 10.18869/acadpub.jafm.67.223.22967.

[4] K. Ali, Y. R. Reddy and B. C. Shekar, Thermo-fluidic transport process in magnetohydrodynamic Couette channel containing hybrid nanofluid, Partial Differential Equations in Applied Mathematics **7** (2023), 100468, DOI: 10.1016/j.padiff.2022.100468.

[5] S. Arrhenius, Über die Reaktionsgeschwindigkeit bei der Inversion von Rohrzucker durch Säuren, *Zeitschrift für Physikalische Chemie* **4U**(1) (1889), 226 – 248, DOI: 10.1515/zpch-1889-0416.

[6] A. R. Bestman, Natural convection boundary layer with suction and mass transfer in a porous medium, *International Journal of Energy Research* **14** (1990), 389 – 396, DOI: 10.1002/er.4440140403.

[7] N. Biswas, N. K. Manna, P. Datta and P. S. Mahapatra, Analysis of heat transfer and pumping power for bottom-heated porous cavity saturated with Cu-water nanoflui, *Powder Technology* **326** (2018), 356 – 369, DOI: 10.1016/j.powtec.2017.12.030.

[8] J. Bodduna, M. P. Mallesh, C. S. Balla and S. A. Shehzad, Activation energy process in bioconvection nanofluid flow through porous cavity, *Journal of Porous Media* **25**(4) (2022), 37 – 51, DOI: 10.1615/JPorMedia.2022040230.

[9] J. Buongiorno, Convective transport in nanofluids, *ASME Journal of Heat and Mass Transfer* **128**(3) (2006), 240 – 250, DOI: 10.1115/1.2150834.

[10] S. U. S. Choi and J. A. Eastman, *Enhancing Thermal Conductivity of Fluids with Nanoparticles*, Technical Report ANL/MSD/CP-84938, CONF-951135-29, Argonne National Lab., Lemont, IL, USA (1995), URL: https://ecotert.com/pdf/196525_From_unt-edu.pdf.

[11] M. Ghalambaz, A. Doostani, E. Izadpanahi and A. J. Chamkha, Conjugate natural convection flow of Ag–MgO/water hybrid nanofluid in a square cavity, *Journal of Thermal Analysis and Calorimetry* **139** (2020), 2321 – 2336, DOI: 10.1007/s10973-019-08617-7.

[12] R. S. R. Gorla, B. Vasu and S. Siddiqa, Transient combined convective heat transfer over a stretching surface in a non-newtonian nanofluid using Buongiorno's model, *Journal of Applied Mathematics and Physics* **4**(2) (2016), 443 – 460, DOI: 10.4236/jamp.2016.42050.

[13] M. R. Hajmohammadi, Cylindrical Couette flow and heat transfer properties of nanofluids; single-phase and two-phase analyses, *Journal of Molecular Liquids* **240** (2017), 45 – 55, DOI: 10.1016/j.molliq.2017.05.043.

[14] G. Huminic and A. Huminic, Hybrid nanofluids for heat transfer applications – A state-of-the-art review, *International Journal of Heat and Mass Transfer* **125** (2018), 82 – 103, DOI: 10.1016/J.IJHEATMASSTRANSFER.2018.04.059.

[15] M. E. Karim, M. A. Samad and M. Ferdows, Numerical study of the effect of variable viscosity on unsteady pulsatile nanofluid flow through a Couette channel of stretching wall with convective heat transfer, *AIP Conference Proceedings* **2121**(1) (2019), 070005, DOI: 10.1063/1.5115912.

[16] K. Khanafer and K. Vafai, Applications of nanofluids in porous medium, *Journal of Thermal Analysis and Calorimetry* **135** (2019), 1479 – 1492, DOI: 10.1007/s10973-018-7565-4.

[17] D. Madhesh, R. Parameshwaran and S. Kalaiselvam, Experimental investigation on convective heat transfer and rheological characteristics of Cu–TiO$_2$ hybrid nanofluids, *Experimental Thermal and Fluid Science* **52** (2014), 104 – 115, DOI: 10.1016/j.expthermflusci.2013.08.026.

[18] M. Mahmoodi and S. Kandelousi, Effects of thermophoresis and Brownian motion on nanofluid heat transfer and entropy generation, *Journal of Molecular Liquids* **211** (2015), 15 – 24, DOI: 10.1016/j.molliq.2015.06.057.

[19] O. D. Makinde and O. Franks, On MHD unsteady reactive Couette flow with heat transfer and variable properties, *Central European Journal of Engineering* **4** (2014), 54 – 63, DOI: 10.2478/s13531-013-0139-0.

[20] O. Manca, S. Nardini and D. Ricci, A numerical study of nanofluid forced convection in ribbed channels, *Applied Thermal Engineering* **37** (2012), 280 – 292, DOI: 10.1016/j.applthermaleng.2011.11.030.

[21] V. Meenakshi, J. Bodduna, M. P. Mallesh and C. S. Balla, Impact of Brownian motion and thermophoresis on entropy generation in a cavity containing microorganisms, *International Journal for Computational Methods in Engineering Science and Mechanics* **24**(4) (2023), 258 – 272, DOI: 10.1080/15502287.2023.2185554.

[22] S. Y. Motlagh and H. Soltanipour, Natural convection of Al$_2$O$_3$-water nanofluid in an inclined cavity using Buongiorno's two-phase model, *International Journal of Thermal Sciences* **111** (2017), 310 – 320, DOI: 10.1016/j.ijthermalsci.2016.08.022.

[23] M. Mustafa, T. Hayat and S. Obaidat, Boundary layer flow of a nanofluid over an exponentially stretching sheet with convective boundary conditions, *International Journal of Numerical Methods for Heat & Fluid Flow* **23**(6) (2013), 945 – 959, DOI: 10.1108/HFF-09-2011-0179.

[24] G. Saha and M. C. Paul, Investigation of the characteristics of nanofluids flow and heat transfer in a pipe using a single phase model, *International Communications in Heat and Mass Transfer* **93** (2018), 48 – 59, DOI: 10.1016/j.icheatmasstransfer.2018.03.001.

[25] M. Sheikholeslami, D. D. Ganji and M. M. Rashidi, Magnetic field effect on unsteady nanofluid flow and heat transfer using Buongiorno model, *Journal of Magnetism and Magnetic Materials* **416** (2016), 164 – 173, DOI: 10.1016/j.jmmm.2016.05.026.

[26] M. A. Sheremet and I. Pop, Free convection in a porous horizontal cylindrical annulus with a nanofluid using Buongiorno's model, *Computers & Fluids* **118** (2015), 182 – 190, DOI: 10.1016/j.compfluid.2015.06.022.

[27] M. A. Sheremet, I. Pop and M. M. Rahman, Three-dimensional natural convection in a porous enclosure filled with a nanofluid using Buongiorno's mathematical model, *International Journal of Heat and Mass Transfer* **82** (2015), 396 – 405, DOI: 10.1016/j.ijheatmasstransfer.2014.11.066.

[28] N. A. C. Sidik, I. M. Adamu, M. M. Jamil, G. H. R. Kefayati, R. Mamat and G. Najafi, Recent progress on hybrid nanofluids in heat transfer applications: A comprehensive review, *International Communications in Heat and Mass Transfer* **78** (2016), 68 – 79, DOI: 10.1016%2Fj.icheatmasstransfer.2016.08.019.

[29] L. S. Sundar, M. K. Singh and A. C. Sousa, Enhanced heat transfer and friction factor of MWCNT–Fe$_3$O$_4$/water hybrid nanofluids, *International Communications in Heat and Mass Transfer* **52** (2014), 73 – 83, DOI: 10.1016/j.icheatmasstransfer.2014.01.012.

[30] R. K. Tiwari and M. K. Das, Heat transfer augmentation in a two-sided lid-driven differentially heated square cavity utilizing nanofluids, *International Journal of Heat and Mass Transfer* **50**(9-10) (2007), 2002 – 2018, DOI: 10.1016/j.ijheatmasstransfer.2006.09.034.

[31] I. Tlili, N. N. Hamadneh, W. A. Khan and S. Atawneh, Thermodynamic analysis of MHD Couette–Poiseuille flow of water-based nanofluids in a rotating channel with radiation and Hall effects, *Journal of Thermal Analysis and Calorimetry* **132** (2018), 1899 – 1912, DOI: 10.1007/s10973-018-7066-5.

[32] A. Zeeshan, N. Shehzad and R. Ellahi, Analysis of activation energy in Couette-Poiseuille flow of nanofluid in the presence of chemical reaction and convective boundary conditions, *Results in Physics* **8** (2018), 502 – 512, DOI: 10.1016/j.rinp.2017.12.024.